Review and system design framework of photovoltaic-powered water treatment*

Andy Augousti[1,*,†], Olena Lanets[1†], Sahand Hosouli[1,†] and Solomiia Liaskovska[1,†]

[1] *Kingston University, Department of Mechanical Engineering, Faculty of Engineering, Computing and the Environment, Roehampton Vale, London SW15 3DW, United Kingdom*

Abstract

This paper proposes a control-oriented framework for modular drinking-water treatment based on photovoltaic (PV) systems for small households and remote areas. Using hourly SSRD (surface solar radiation downwards) data for Turkey (2025), the study derives two practical solar indicators for operation planning: monthly average daily solar energy and average daily active hours above irradiance thresholds (100 and 200 W/m²). These indicators are linked to a rule-based mode-selection scheme (Modes A/B/C) for treatment planning under seasonal variability of solar resource and PV availability. The framework adopts a reference pre-filtration–UV–clean-water tank chain and uses turbidity as a minimum operational quality gate to support effective UV disinfection. An illustrative household case (150 L/day) and a minimal sensitivity analysis based on the specific energy consumption (SEC) of the process chain show how process energy intensity affects approximate PV sizing. The results provide a practical link from seasonal solar-resource assessment to control-oriented design and operation of PV-powered drinking-water modules.

Keywords

photovoltaic-powered water purification, drinking water module, SSRD

1. Introduction

Access to safe drinking water in small households and remote locations is often limited by unstable infrastructure and power supply. Photovoltaic (PV) power is attractive for such conditions, but has a key engineering limitation: power generation is variable (daily/seasonal), while water treatment must ensure stable quality and predictable water availability. PV-powered approaches to water purification and individual process units (disinfection, membranes, storage, control) are widely discussed in the literature [1, 2, 3, 4]. While our present workflow relies on standard spatiotemporal aggregation of SSRD data, related research highlights that numerical stability and computational acceleration (e.g., regularisation and OpenMP parallelisation) can be important for large-scale scientific computing tasks [5]. However, in practical scenarios for households, a reproducible design procedure is needed that links the solar resource, the household's drinking water demand, and the choice of system modes and configurations.

As a contribution of the article: (1) we propose a framework for designing a modular drinking water system with PV power and storage in a tank – with the proposed contribution of storing (water storage as a more practical and cheaper alternative to storing electricity in batteries); (2) we introduce a rule-based decision table based on seasonal solar resource and active hours above given thresholds (100 and 200); (3) we form a reference architecture for a household (example: 10 people) and describe a set of smart modules for mode management, energy budget and quality control. As a geographical location we have chosen Turkey as this forms part of a British Council funded project

*SmartIndustry 2026: 3rd International Conference on Smart Automation & Robotics for Future Industry, March 26–27 , Lviv, Ukraine

* Corresponding author.

† These authors contributed equally.

augousti@kingston.ac.uk (A. Augousti); O.Lanets@kingston.ac.uk (O. Lanets); s.hosouli@kingston.ac.uk (S. Hosouli), solomiam@gmail.com (S. Liaskovska);

0000-0003-3000-9332 (A. Augousti); 0000-0001-7149-0957 (O. Lanets); 000-0002-1842-1431 (S. Hosouli), 0000-0002-9761-0096 (S. Liaskovska)

to investigate the use of solar PV systems for water purification (Project Reference: 1203750378 Augousti Turkey ‘SunGel’).

2. Scope, definitions, and assumptions

Within the scope of this analysis, we consider only drinking water and systems where PV is the source of electricity for water treatment processes.

By PV-powered drinking water treatment, we mean the following possible configurations:

- off-grid - autonomous operation without a grid, hybrid: PV + additional source/storage.
- grid-tied - PV integrated with the grid.

The key assumption of the framework is that in small drinking water systems it is advisable to minimize battery storage and use a clean water tank as the main buffer, and perform the treatment (’treat-when-sunny’) with adaptation of regimes according to seasonal sun indicators and the active hours above specified thresholds.

According to the requirements for basic water needs for households in remote environments, typical total basic water needs are in the range of 7.5–15 litres per day [6].

For PV-powered drinking water modules, UV disinfection is often a practical final step, but its effectiveness is critically dependent on water clarity. The Drinking Water Inspectorate (DWI) states that UV turbidities should remain below 1 NTU, and for effective disinfection, it is recommended that median turbidity ideally be below 0.2 NTU [7].

DWI also explicitly states the need for pre-filtration before UV, as pre-filtration, capable of providing turbidity <1 NTU, reduces screening of microorganisms by particles and helps reduce UV lamp fouling [8, 9].

Based on this, it is appropriate to adopt a modular pre-filtration/Ultrafiltration-UV-clean water tank chain as the basic 'reference chain' for drinking water in our framework, where the tank (water storage) acts as a product accumulator.

For Turkey, in a water source context, it is appropriate to consider surface water and groundwater as the main classes of raw water, where the total usable water potential is 112 billions of cubic metres (BCM)/yr, of which 94 BCM is surface water and 18 BCM is groundwater [10].

Brackish/seawater can be left as a separate scenario, as it usually involves a different technological chain and a significantly different energy intensity.

This study focuses on a practical design gate for PV-powered drinking-water modules rather than a full regulatory compliance assessment. Microbiological compliance targets (e.g., E. coli) and dissolved-solids criteria (e.g., Total dissolved solids, Electrical conductivity) are not parameterised in the present framework. Instead, we adopt turbidity as a minimum operational quality gate to ensure effective UV disinfection.

Photovoltaic power for modular drinking water systems can be based on different PV technology families, including crystalline silicon (c-Si), thin-film modules (e.g. CdTe and CIGS/CIS) and high-efficiency III–V cells (e.g. GaAs on a Ge substrate). Commercial c-Si technologies typically have conversion efficiencies in the range of 20–25%, while III–V cells can reach 25–30% (without concentration), but due to their high cost, they are mostly used in niche applications such as space. It is important that the PV cells are connected and encapsulated in a PV module, and at the system level, ancillary components (mounting, power electronics and control) need to be considered. In off-grid solutions, batteries are often used, but for some applications — in particular, water pumping — a battery-free mode is possible, when energy is consumed as it is generated. This justifies the concept of drinking water modules with a ‘treat-when-sunny’ mode and the accumulation of purified water in a tank [11].

3. Methods

3.1. Study data and preprocessing

The analysis uses the year 2025 (8760 time steps) on a regular 0.25° latitude–longitude grid [12], with Turkey extracted using a country boundary mask (GADM) [13]. We used the Surface Solar Radiation Downwards (SSRD) variable, provided as accumulated energy per unit area (J/m²) on an hourly time grid for 2025 [14]. The accumulation period was obtained directly from the time coordinate step (t=3600 s). Mean irradiance was computed in W/m², as

$$G(t) = SSRD(t) / \Delta t . \quad (1)$$

Active time steps were defined as those with $SSRD(t)>0$, representing periods with non-zero incoming shortwave radiation. Spatial summaries for Turkey were computed as the grid-mean over masked cells, and temporal summaries were produced via daily aggregation and monthly means for seasonal comparison.

3.2. Solar indicators for PV-driven operation

To characterise the solar resource in a form that is directly useful for operating a PV-powered treatment module, we use two complementary indicators derived from *SSRD*. Seasonal resource is expressed as the monthly average daily solar energy (kWh/m²/day), which summarises long-term seasonal variability and provides a first-order estimate of the energy available per unit PV area. Availability was quantified as the average number of hours per day during which the derived irradiance $G(t)$ exceeded two operational thresholds (100 and 200 W/m²) [15]. Threshold-based time windows are commonly used to define PV production/availability periods. The 100 W/m² level is consistent with irradiance filtering practices used in PV performance analyses, while 200 W/m² provides a stricter high-resource availability indicator. The lower threshold represents low but usable solar conditions, while the higher threshold represents periods of stronger irradiance more suitable for energy-demanding operation. Together, these indicators act as operational proxies for planning the duty cycle and selecting operating modes under intermittent and seasonal PV supply.

3.3. Framework for mode selection and modular treatment design

In addition to seasonal solar energy, we quantify operational availability as the average number of active hours per day during which the derived irradiance exceeds 100 W/m² and 200 W/m². These thresholds are used as operational proxies to distinguish between weaker and stronger PV operating windows: hours/day above 100 W/m² indicate time windows suitable for low-power or batch operation, whereas hours/day above 200 W/m² represent periods more favourable for energy-intensive or more continuous pumping cycles. Table 1 presents the functional decomposition of the proposed PV-driven drinking-water control framework, showing how resource indicators and sensor signals are translated into rule-based operating actions (Modes A/B/C, storage control, and interlocks).

Table 1
Control-oriented modular architecture for PV-driven drinking-water operation

Module (function)	Inputs (signals/data)	Logic / decision rule	Outputs (actuation / setpoints)	Key parameters
M1. Mode manager (A/B/C)	Monthly indicators (H_m, h_{100}, h_{200}); optional	Rule-based mode selection (A/B/C)	Selected mode label; priority schedule (e.g., pump-first vs	Switching thresholds; hysteresis band;

	demand target *Vd* (L/day)	based on seasonal resource and availability; hysteresis to avoid rapid switching	UV-first); target duty-cycle bounds; minimum storage reserve	scheduling window (days); minimum runtime per mode
M2. PV input trigger (real-time gating)	Real-time irradiance *G(t)* (W/ m^2) derived from *SSRD*, or PV power sensor *PV(t)* (W)	Enables/ disables treatment and pumping when PV input exceeds configured start/stop thresholds; optional soft-start/ ramp logic to reduce switching stress	Permit signals for pump/UV; start/stop commands; PV-available status flag	G_{start}, G_{stop} (or P_{start}, P_{stop}); debounce time; optional minimum ON/OFF time
M3. Clean-water tank storage controller (product accumulator)	Clean-tank level L_{tank} (L or % of usable volume); tank inflow status; demand draw status (optional).	if $L_{tank} \leq L_{min}$, issue a production request; if $L_{tank} \geq L_{max}$, stop the production request (tank full condition). A hysteresis band (L_{min}, L_{max}) is used to avoid rapid switching.	Production request; enable/disable request to upstream treatment modules (subject to PV gating in M2); low-storage alarm/warning.	L_{min}, L_{max}, seasonal reserve target L_{res} (optional), usable tank volume V_{tank} (design variable).
M4. Quality gate (turbidity for UV feasibility)	turbidity before UV / before clean tank (NTU)	if turbidity exceeds UV suitability limits → block transfer to clean tank and/or enforce pre-	turbidity limits (NTU)	UV suitability requires low turbidity; pre-filtration recommend

		filtration loop interlock no transfer to clean tank; bypass/recirculation command; maintenance flag		ed by DWI
M5. UV and flow safety interlock	flow switch, pump-run signal, UV status UV ON only when flow is present;	emergency stop if no flow; optional UV warm-up/monitoring	UV enable; fault flag; safe shutdown	minimum flow threshold, timeout, UV warm-up time

Note: Exact numerical thresholds for M2/M3/M5 are system-specific (pump curve, hydraulics, UV reactor design) and are therefore treated as tunable parameters rather than universal constants. Mode A: low-resource / batch treatment (tank-led, duty-cycled). Mode B: moderate-resource / mixed operation. Mode C: high-resource / near-continuous pumping/treatment.

L_{tank}, L_{min}, and L_{max} denote the clean-water tank level and switching thresholds in litres (L); V_{tank} is the usable tank volume (L). Turbidity T is measured in NTU, and the turbidity gate is defined by threshold T_{max} (NTU), which blocks transfer to the clean-water tank when exceeded. Transfer to the clean-water tank is permitted only if $T \leq 1$ NTU; the recommended target is median turbidity ≈ 0.2 NTU.

3.4. Algorithm

We implement a data-driven mode selection rule based on the monthly availability indicator h200(m), defined as the monthly mean of hours per day with irradiance $G(t)$>200 W/m^2 (Turkey grid-mean). The 25th and 75th percentiles of the 12 monthly values are used as thresholds (P_{25} and P_{75}). For 2025, the computed thresholds are P_{25} = 3.734 h/day and P_{75} = 5.798 h/day. Months with $h_{200}(m)$<P25 are assigned to Mode A (low-resource operation), months with $h_{200}(m) > P_{75}$ to Mode C (high-resource operation), and the remaining months to Mode B (intermediate resource).

Applying this rule to the 2025 dataset yields: Mode A in January, November, and December; Mode C in May–July; and Mode B in the remaining months (February–April, August–October). (Table 2)

Table 2
Mode assignment based on monthly h_{200}, using percentile thresholds P_{25} and P_{75}.

Month (2025)	h_{200} (h/day)	Mode
Jan	3.139	A
Feb	3.827	B
Mar	4.756	B
Apr	5.161	B

May	5.815	C
Jun	6.329	C
Jul	6.219	C
Aug	5.793	B
Sep	5.082	B
Oct	4.164	B
Nov	3.456	A
Dec	2.551	A

4. Results

Primary solar indicators were generated in Google Colab (Python) from Copernicus CDS/ERA5 data (SSRD). Hourly average irradiance was calculated as

$$G = SSRD/3600, \quad (2)$$

then 'useful solar hours' were defined as the number of hours when G>100 W/m² and G>200 W/m² and aggregated to monthly averages. The summary tables were exported and visualized in Colab (Fig.1–Fig.3).

Figure 1 shows the spatial distribution of the average *SSRD* over Turkey, calculated for the year 2025 with the time axis valid_time from 2025-01-01 00:00 to 2025-12-31 23:00 (8760 steps in total). In order to consider only the moments with real solar energy input, active time steps are defined as those where *SSRD* > 0 and the average is calculated only over these steps. The map shows higher values in the southern latitudes of Turkey and lower values in the northern latitudes, which is consistent with the latitudinal variation of insolation.

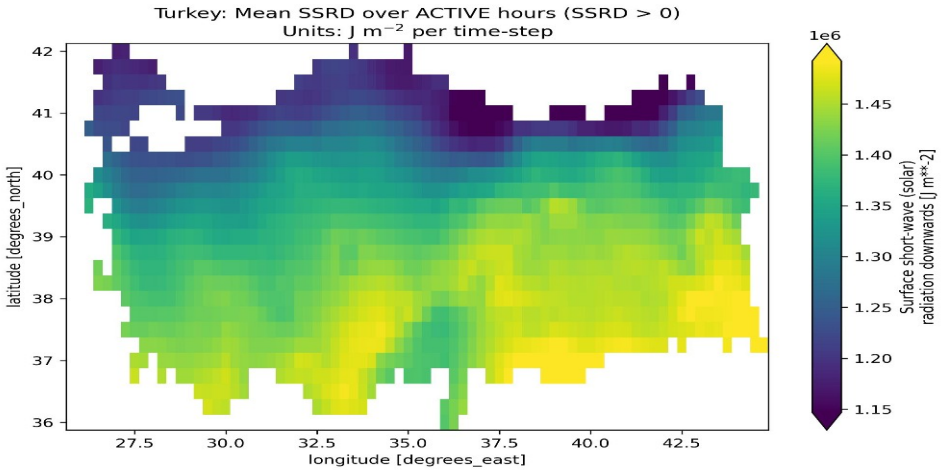

Figure 1: Turkey: mean *SSRD* during active time steps (*SSRD*>0), 2025; units J/m² per time step.

Figure 2 summarises the seasonal variability of the solar resource over Turkey in 2025. The grid-mean average daily solar energy increases from 1.704 kWh/m²/day (January) to a peak of 5.243

kWh/m²/day (June), then declines towards 1.338 kWh/m²/day (December). This seasonal pattern indicates that PV-powered treatment systems in Turkey are likely to experience higher operating margins in late spring and summer and tighter constraints in winter, motivating storage and/or adaptive operating modes.

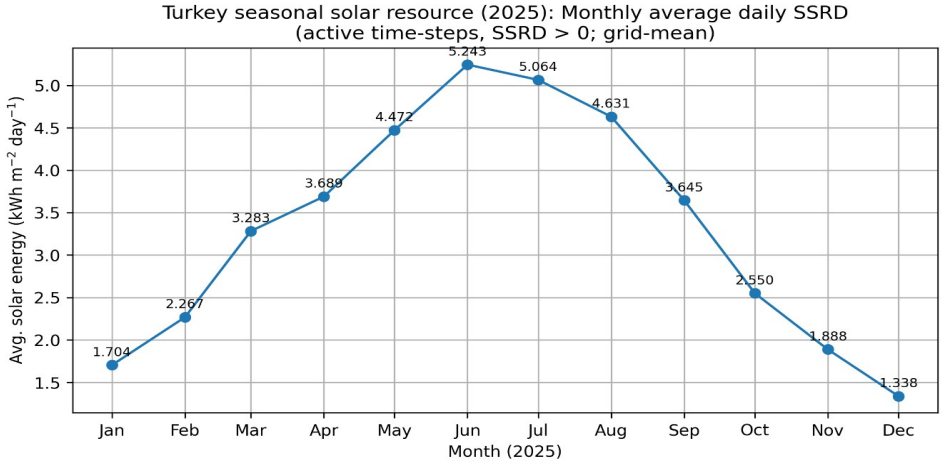

Figure 2: Turkey seasonal solar resource (2025): monthly average daily SSRD during active time steps.

Figure 3 quantifies the seasonal availability of useful solar hours over Turkey in 2025. The country-average number of hours per day above 100 W/m² rises from winter to a summer maximum, while the stricter 200 W/m² threshold yields fewer available hours across all months, reflecting periods of stronger irradiance that are more suitable for energy-intensive treatment modes. Irradiance was derived from *SSRD* (surface short-wave radiation downwards) by converting energy per time step to power as

$$G(t) = SSRD / \Delta t, \tag{3}$$

where the dataset time step being 3600 s. Only grid cells inside the Turkey boundary mask were included.

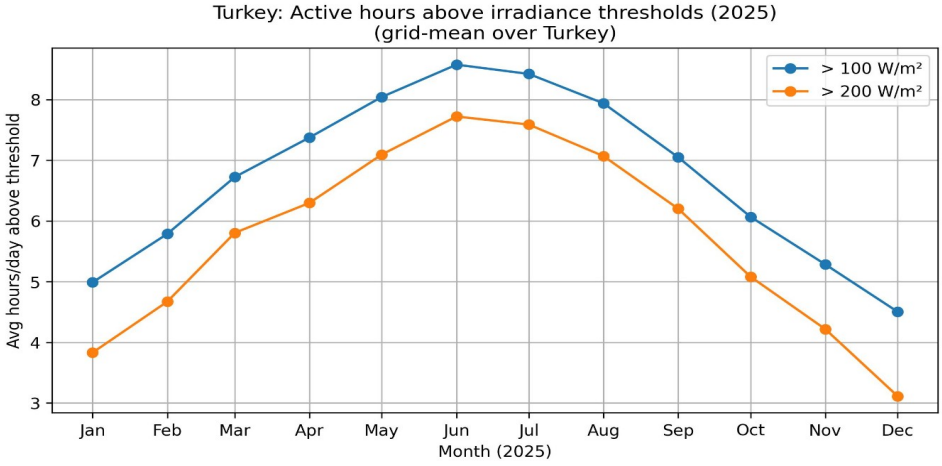

Figure 3: Turkey: average daily hours above irradiance thresholds (2025).

The seasonal input variables of the decision table are formed from the climate/solar data: Monthly Energy (kWh/m²/day) and the average number of active hours per day above the thresholds of 100 W and 200 W (Fig. 2-3).

The runtime input signals are used to implement the rules in real time: a trigger for sufficient PV power/irradiance (e.g., PV power/irradiance sensor), the water level in the tank, and quality gate signals (e.g., turbidity before UV) to block the water supply to the clean water tank in case of inadequate quality.
The rules for selecting the seasonal mode (planning layer):
Mode A (low-power / winter mode): if hours/day >200 W are low, but hours/day >100 W are available, the system selects low-power operations and batch cleaning, with the priority of maintaining a minimum reserve in the tank.
Mode B (standard/shoulder seasons): at average Monthly Energy values and moderate hours/day >200 W, the system switches to regular pumping cycles with UV disinfection, maintaining a stable tank filling.
Mode C (high-throughput / summer mode): at high Monthly Energy values and high hours/day >200 W, the system operates at maximum throughput, quickly filling the tank and creating a reserve for periods of lower resource.
Runtime layer rules: within the selected seasonal mode, the system starts a cleaning cycle only when (i) the PV input is sufficient (power/irradiance threshold trigger is triggered) and (ii) the tank needs to be refilled (tank level below a given level).
Quality gate for UV is mandatory regardless of the mode: UV disinfection efficiency requires low turbidity (turbidity <1 NTU, ideally ~0.2 NTU) and appropriate pretreatment; therefore, water supply to the clean water tank is only allowed if this condition is met.
In the literature, start/stop thresholds and control rules for PV water systems are often specified for a specific configuration (pump-PV-hydraulics) and may be formulated as thresholds in terms of irradiance or available PV power, while other configurations give significantly different threshold values. For a direct PV pump system, irradiance thresholds for start/stop are given in the literature, e.g. GI_{thre_start} = 300 W/m² and GI_{thre_stop} = 200 W/m². Other works show that the threshold can vary significantly depending on the configuration and control algorithm [16, 17, 18].

4.1. Illustrative case study and sensitivity: reference household module

We consider a reference household of 10 people and adopt a minimum daily water demand of 15 L/person/day, i.e. 150 L/day (0.15 m³/day).
The reference treatment chain is pre-filtration → UV disinfection, and a clean-water tank is introduced to decouple treatment (during hours of sufficient solar resource) from consumption.
A practical design choice is a tank volume of 150–300 L, corresponding to approximately 1–2 days of autonomy at 150 L/day.
Energy balance parameterisation. The daily electrical energy requirement is parameterised using the specific energy consumption *SEC* (kWh/m³) of the selected process chain is

$$E_{day} = V_d \cdot SEC \tag{4}$$

where V_d=0.15 m³/day.

PV yield is estimated from the monthly average daily solar energy H_m (where m denotes month) (kWh/ m² /day) as

$$E_{PV,day} = H_m \cdot \eta_{PV} \cdot PR \cdot A, \tag{5}$$

where H_m is the monthly average daily solar energy (kWh /m² /day), A is PV area (m²), η_{PV} is module efficiency, and PR is the performance ratio accounting for system losses.

Combining these expressions gives the PV area required to meet the daily energy need is

$$A = V_d \cdot SEC / H_m \eta_{PV} PR. \tag{6}$$

As a minimal sensitivity analysis, we vary *SEC* to demonstrate how PV sizing scales with process energy intensity without introducing detailed pump models. For an illustrative winter design month, we use H_m=1.338 kWh/m²/day, and adopt representative PV performance parameters

η_{PV}=0.20 and *PR*=0.75. For the reference demand of 150 L/day ($\underline{V_d}$=0.15 m³/day), three *SEC* scenarios (0.5, 1.0, and 2.0 kWh /m³) yield daily energy needs of 0.075, 0.150, and 0.300 kWh/day, corresponding to PV areas of approximately 0.374, 0.747, and 1.495 m², respectively. Reporting convenience, the equivalent PV rated peak power (nameplate capacity, Wp) is estimated as $W_p \approx A \cdot 1000 \cdot \eta_{PV}$, giving about 75, 149, and 299 Wp for the three scenarios. The results show a linear dependence of PV area on *SEC*. Therefore, for a fixed water demand, the assumed process energy intensity is a dominant driver of PV sizing.

To make this section fully reproducible with fewer assumptions, the following inputs should be fixed explicitly: (i) the winter design-month value of Hm taken directly from Fig. 2 (or from a table of monthly values), and (ii) the PV performance parameters (η_{PV} and *PR*) chosen for the study either as representative assumptions or as technology-specific values. If pumping is modelled explicitly, additional pump parameters (head, flow, and efficiency) or an equivalent pumping-energy contribution expressed in kWh/m³ are required.

PV sizing is estimated using a simplified daily energy balance. We adopt representative PV performance parameters for the illustrative sizing calculation: η_{PV}=0.20, consistent with reported commercial crystalline-silicon efficiencies, and *PR*=0.75, within typical *PR* ranges for PV systems [19]. Daily electricity demand is parameterised via the specific energy consumption of the selected process chain.

Results show a linear scaling: increasing *SEC* from 0.5 to 2.0 kWh/m³ increases the required PV area from ~0.37 to ~1.49 m² (≈75 to 299 Wp), highlighting that process energy intensity is a dominant driver of PV sizing for fixed water demand. (Table 3)

Table 3
Sensitivity of PV sizing to process energy intensity (SEC) for a 150 L/day reference demand (0.15 m³/day)

SEC (kWh/m³)	E_day (kWh/day)	PV area A (m²)	PV size (Wp)
0.5	0.075	0.37	74.74
1.0	0.15	0.75	149.48
2.0	0.3	1.49	298.95

5. Discussion

The results emphasise that PV variability is not only a question of how much energy is generated per month, but also of how long the power window is usable for a given duty cycle. The combined use of monthly average daily solar energy (Figure 2) and average active hours above 100 and 200 W/m^2 (Figure 3) converts a climatological resource into control-oriented indicators. In particular, seasonal bottlenecks emerge when H_m is low and h_{200} shrinks, even if the system can operate intermittently, the reduced high-irradiance window limits continuous pumping and energy-intensive cycles, which pushes operation toward Mode A (batch/low-power) and increases reliance on buffering. Conversely, months with consistently higher h_{200} support Mode C-like operation, where longer cycles and higher daily productivity are feasible with less aggressive scheduling.

A second, non-negotiable bottleneck is raw-water quality prior to UV. DWI guidance highlights that effective UV disinfection requires low turbidity and appropriate pre-filtration, since suspended particles can shield microorganisms and contribute to UV lamp fouling. In control terms, this motivates a turbidity-gate: the system should only permit transfer to the clean-water tank when turbidity conditions compatible with UV efficacy are satisfied. This shifts quality from being an offline specification to an explicit operational constraint that can override energy availability.

These bottlenecks motivate storage as an architectural response to intermittency. In line with battery-free 'use-as-generated' approaches in off-grid PV-water applications, water storage in a clean tank can decouple treatment, performed during sufficient solar windows, from demand (served from storage). This framing also aligns with the recognised tank vs battery trade-off. Storage can be provided in the hydraulic domain (tank autonomy) rather than in the electrical domain (battery capacity), depending on the desired reliability, complexity, and maintenance constraints.
Finally, the 10-person reference demand (150 L/day) provides a transparent and reproducible design scale for linking seasonal resource indicators to operational modes and tank sizing. At the same time, PV sizing should be interpreted as configuration-dependent. It is governed primarily by the process *SEC* and system losses, and should therefore be reported together with the assumed *SEC* and PV performance parameters when used for illustrative calculations.

6. Conclusions

The article proposes a control-oriented framework for PV-powered drinking-water modules that links seasonal solar resource to rule-based operating modes (A–C). Using hourly SSRD for Turkey (2025), we derive monthly energy and active hours above 100/200 W/m^2 as operational proxies for scheduling and mode selection. UV disinfection is treated as a quality-constrained operation: low turbidity and pre-filtration requirements justify a turbidity gate before clean-water storage. Tank storage is presented as a practical buffer enabling 'treat-when-sunny' operation and reducing reliance on batteries. A 10-person reference demand (150 L/day) provides a transparent design scale, and a minimal sensitivity analysis shows PV sizing scales linearly with SEC.
Future work should parameterise an end-to-end configuration (SEC for the chosen treatment chain, pump head–flow–efficiency, and power-electronics/control losses) to convert the present rule-based modes into calibrated numerical thresholds and to validate productivity and reliability under representative demand profiles.

Acknowledgements

This work was supported by funding from a British Council International Science Partnership Fund project (Project Reference: 1203750378 Augousti Turkey ‘SunGel’), and two of the authors were also supported by funding from the British Academy Researchers at Risk Programme and the Researchers at Risk Programme Extension, OL (Ref: RaR\100790 and RaR\100266) and SL (Ref: RaR\100791 and RaR\100190).

Declaration on Generative AI

During the preparation of this work, the author(s) used AI tools in order to: Grammar and spelling check.

References

[1] Li, S., Cai, Y.-H., Schäfer, A.I., Richards, B.S.: Renewable energy powered membrane technology: A review of the reliability of photovoltaic-powered membrane system components for brackish water desalination. Applied Energy 253, 113524 (2019). https://doi.org/10.1016/j.apenergy.2019.113524

[2] Soenen, C., Reinbold, V., Meunier, S., Cherni, J.A., Darga, A., Dessante, P., Quéval, L.: Comparison of Tank and Battery Storages for Photovoltaic Water Pumping. Energies 14(9), 2483 (2021). https://doi.org/10.3390/en14092483

[3] Hennache, A., Quamar, M.M., Khan, K.A., Alqahtani, M., Ahmed, I., Khalid, M.: Control strategies for reverse osmosis desalination powered by photovoltaic systems: A comprehensive review. Energy Strategy Reviews 62, 101944 (2025). https://doi.org/10.1016/j.esr.2025.101944

[4] García-Gil, Á., García-Muñoz, R.A., McGuigan, K.G., Marugán, J.: Solar Water Disinfection to Produce Safe Drinking Water: A Review of Parameters, Enhancements, and Modelling Approaches to Make SODIS Faster and Safer. Molecules 26(11), 3431 (2021). https://doi.org/10.3390/molecules26113431
[5] Mochurad, L., Shakhovska, K., Montenegro, S.: Parallel Solving of Fredholm Integral Equations of the First Kind by Tikhonov Regularization Method Using OpenMP Technology. In: Shakhovska, N., Medykovskyy, M.O. (eds) Advances in Intelligent Systems and Computing IV (CSIT 2019), AISC, vol. 1080, pp. 25–35. Springer, Cham (2020). doi:10.1007/978-3-030-33695-0_3
[6] The Sphere Project: Humanitarian Charter and Minimum Standards in Disaster Response. The Sphere Project, Geneva, 2004. ISBN 92-9139-097-6. Available at: https://sphereprototype.conted.ox.ac.uk/sphereprototype.conted.ox.ac.uk/standards/watersupply/accessAndWaterQuantity.html#
[7] DWI: Guidance on the use of ultraviolet (UV) irradiation for the disinfection of public water supplies. URL: https://www.dwi.gov.uk/private-water-supplies/pws-installations/uv-systems (accessed: 22 Jan. 2026).
[8] Drinking Water Inspectorate (DWI): UV disinfection. Private water supplies: Treatment guide. Online resource. Available at: https://www.dwi.gov.uk/private-water-supplies/pws-installations/treatment-guide-2/uv-disinfection/ (accessed: 30 Jan 2026).
[9] Turkish Water Institute (SUEN): Turkey and Water. Turkish Water Institute (SUEN), Ankara, 2018. Available at: https://www.suen.gov.tr/uploads/turkey-and-water.pdf (accessed: 30 Jan 26).
[10] Fanack Water: Water Resources in Turkey. 2022. URL: https://water.fanack.com/turkey/water-resources-in-turkey/ (accessed: 22 Jan. 2026).
[11] IEA PVPS T1-48:2025, Trends in Photovoltaic Applications 2025, International Energy Agency Photovoltaic Power Systems Programme (IEA PVPS), 2025. URL: https://iea-pvps.org/wp-content/uploads/2025/10/IEA-PVPS_Trends_2025-.pdf
[12] Hersbach, H., Bell, B., Berrisford, P., et al.: The ERA5 global reanalysis. Quarterly Journal of the Royal Meteorological Society 146(730), 1999–2049 (2020). https://doi.org/10.1002/qj.3803
[13] GADM: Database of Global Administrative Areas (GADM), version 4.1. Available at: https://geodata.ucdavis.edu/gadm/gadm4.1/ (accessed: 23 Jan 2026).
[14] Copernicus Climate Change Service (C3S): ERA5 reanalysis (single levels). Climate Data Store (CDS). Available at: https://cds.climate.copernicus.eu/datasets/reanalysis-era5-single-levels (accessed: 23 Jan 2026).
[15] Lindig, S., Moser, D., Curran, A.J., Rath, K., Khalilnejad, A., French, R.H., Herz, M., Müller, B., Makrides, G., Georgiou, G., Livera, A., Richter, M., Ascencio-Vásquez, J., van Iseghem, M., Meftah, M., Jordan, D., Deline, C., Sark, W.G.J.H.M. van, Stein, J.S., Theristis, M., Meyers, B., Baumgartner, F., Luo, W.: International collaboration framework for the calculation of performance loss rates: Data quality, benchmarks, and trends (towards a uniform methodology). Prog. Photovolt. Res. Appl. 29(6), 573–602 (2021). https://doi.org/10.1002/pip.3397
[16] Orts-Grau, S., González-Altozano, P., Gimeno-Sales, F.J., Balbastre-Peralta, I., Martínez Márquez, C.I., Gasque, M., Seguí-Chilet, S.: Photovoltaic Water Pumping: Comparison Between Direct and Lithium Battery Solutions. IEEE Access 9, 101147–101163 (2021).
[17] Carricondo-Antón, J.M., Jiménez-Bello, M.A., Juárez, J.M., et al.: Optimization of an isolated photovoltaic water pumping system with technical–economic criteria in a water users association. Irrigation Science 41, 817–834 (2023). https://doi.org/10.1007/s00271-023-00859-6
[18] Kumarasamy, S., Narasimhan, S., Narasimhan, S.: Optimal operation of battery-less solar powered reverse osmosis plant for desalination. Desalination 375, 89–99 (2015). https://doi.org/10.1016/j.desal.2015.07.029

[19] Dierauf, T., Growitz, A., Kurtz, S., Cruz, J.L.B., Riley, E., Hansen, C.: Weather-Corrected Performance Ratio. Technical Report NREL/TP-5200-57991, National Renewable Energy Laboratory (NREL), April 2013. URL: https://docs.nrel.gov/docs/fy13osti/57991.pdf